https://doi.org/10.5194/egusphere-2026-1019
Preprint. Discussion started: 10 March 2026

Diurnal cycles of cloud and rainfall over North–East Queensland during the coral bleaching season

Alanah Chapman[1,2,3], Yi Huang[1,4], and Claire Vincent[1,4]

[1]School of Geography, Earth and Atmospheric Sciences, The University of Melbourne
[2]ARC Centre of Excellence for Climate Extremes, Melbourne, VIC, Australia
[3]CSIRO Environment, Melbourne, Australia
[4]ARC Centre of Excellence for 21st Century Weather, Melbourne, VIC, Australia

Correspondence: Yi Huang (yi.huang4@unimelb.edu.au)

Abstract. Mass coral bleaching events are becoming increasingly frequent over the Great Barrier Reef, posing a critical risk to Australia's marine ecosystems and the broader global ocean environment. These events are primarily driven by anomalously warm water temperatures, but their severity is strongly influenced by local cloud cover, which controls the amount of solar radiation reaching the ocean surface (including ultra–violet radiation which exacerbates bleaching). This study presents a characterization of the cloud and rainfall diurnal cycles over north–east Queensland during the coral bleaching season, providing a foundational step to untangling the complex relationships between clouds, rainfall, local–scale processes and the surface energy budget for this climate–sensitive region. Leveraging high–resolution Himawari–8 satellite brightness temperature data, C–band radar observations, and BARRA–R2 regional reanalysis, a multi–year analysis is conducted across three representative zones: coastal land, coastal ocean and open ocean. Results show that diurnal cycles vary distinctly by region and are strongly modulated by prevailing wind regimes. In general, westerly regimes are associated with clear skies and stronger daytime heating over the coastal ocean with enhanced convection over coastal land. In contrast, the frequently observed southeasterlies lead to relatively weaker development over the land and ocean. Cloud and rainfall maxima exhibit out–of–phase behavior between land and ocean, with rainfall often preceding cold cloud tops, indicative that cold brightness temperatures frequently correspond to decaying anvils rather than active convection. Latitudinal and topographic differences contribute to more intense convection near Cairns than Townsville. Variations in inland versus offshore propagation speeds further highlight regional complexity. Our findings emphasize the necessity for high–resolution simulations to advance understanding of convection initiation and propagation mechanisms.

1 Introduction

Variations in the diurnal cycles of clouds over tropical regions significantly influences rainfall variability and regional heat and energy budgets. The relationship between local–scale cloud cover and radiation is a key factor modulating the Sea Surface Temperatures (SSTs) over the Great Barrier Reef (GBR) (Huang et al., 2024; McGowan and Theobald, 2023; Richards et al., 2024; Zhao et al., 2021). With anomalously warm SSTs recognized as the main driver of thermal coral bleaching events (CBEs),

https://doi.org/10.5194/egusphere-2026-1019
Preprint. Discussion started: 10 March 2026

understanding the multi–scale variability in cloud cover over this region is a crucial step towards a quantitative understanding of the ocean heat budget.

Driven by the daily cycle of solar heating, diurnal cycles not only impact local and regional weather, but can also contribute to non–linear upscale processes which can influence the global climate (Masson et al., 2012; Slingo et al., 2003). This effect is particularly pronounced in the deep tropics where diurnally forced convection and rainfall accounts for roughly 50% of mean rainfall and strongly interact with the Madden–Julian Oscillation (MJO) (Birch et al., 2016; Love et al., 2011; Rauniyar and Walsh, 2011). Global transport of moisture and energy is intricately linked to tropical variability, prompting extensive research on diurnal cycles, particularly over the Maritime Continent (MC). However, climate models continue to systematically underestimate mean convection and rainfall in the tropics, often due to misrepresentation of the diurnal cycle. These persistent shortcomings underscore the critical need to understand local–scale convective processes, particularly in under–studied regions such as northeast Queensland, Australia (Birch et al., 2016; Love et al., 2011; Neale and Slingo, 2003).

Diurnal cycles of clouds and rainfall over tropical coastal land regions, particularly in the nearby MC, typically peak during the afternoon–to early evening (Hassim et al., 2016; Mori et al., 2004; Vincent and Lane, 2016; Yang and Slingo, 2001; Lopez-Bravo et al., 2023b). These patterns are shaped by local–scale processes such as sea and valley breezes, and boundary layer mixing, which are further influenced by local topography and large–scale background wind fields. Convection that develops over land during the day often propagates offshore during the evening and night, leading to peak cloudiness and rainfall over adjacent ocean areas during the late evening to early morning hours (Yang and Slingo, 2001; Lopez-Bravo et al., 2023b). High–resolution simulations show that offshore propagation can extend up to 700 km (Vincent and Lane, 2016), and is associated with two distinct mechanisms: slow–moving density currents associated with the land and mountain breezes near–shore, and faster–traveling gravity waves beyond 200 km from the coastline (Mapes et al., 2003). While these patterns represent typical diurnal behavior in tropical coastal and marine environments, significant regional variations exist (Lopez-Bravo et al., 2023b; Peatman et al., 2023; Yokoi et al., 2017). Therefore, it is essential to characterize the diurnal cycles of clouds and rainfall specific to the GBR region, which spans both tropical and subtropical zones. Such characterization is important for improving our understanding of the local heat and energy budgets, particularly during the periods relevant to coral bleaching.

Understanding the diurnal variability of local cloud and rainfall cycles is crucial for uncovering how cloudiness interacts with surface energy fluxes, and for identifying the processes that govern these exchanges. Vincent and Huang (2022) examined the relationship between local morning insolation and the diurnal rainfall cycle for three forested sites in the MC. They found that higher morning insolation is associated with increased afternoon rainfall over land, and that this was poorly captured in convection–permitting model simulations. Beyond the MC, relatively few studies have explored how diurnal cycles of clouds and rainfall interact with the boundary layer and surface fluxes. May et al. (2012) used data from the international Tropical Warm Pool International Cloud Experiment (TWP–ICE) and weather radar (among other instruments) to investigate the effects of convective rainfall on surface radiation in a coastal monsoon setting. Their findings showed that the shortwave (SW) cloud effects dominated net surface radiation fluxes, with up to three times more energy reaching the surface during periods of large–scale suppressed conditions. In contrast, during the monsoonal period, increased cloud optical thicknesses and persistent high–level clouds significantly reduced net surface radiation by blocking incoming SW radiation. Direct in situ measurements

https://doi.org/10.5194/egusphere-2026-1019
Preprint. Discussion started: 10 March 2026

of the surface energy balance are far more common over land than ocean, largely due to the logistical challenges of instrument setup and maintenance in marine environments. In the southern GBR, a case study by McGowan et al. (2010) examined the surface energy balance using in situ measurements. They found that 80–98% of net daytime radiation reaching the ocean surface contributed to heating of shallow reef flats. Although their observations were limited to spring and winter, the study highlighted the critical role of cloud cover in modulating the ocean heat budget.

In the context of the GBR, Zhao et al. (2021) provided a broad characterization of seasonal cloud properties across large spatial scales. However, fine–scale diurnal variability — poorly captured by both Numerical Weather Prediction and climate models — remains largely unexamined. This gap is critical, given the significant effects of diurnal radiative cloud forcings on surface radiative fluxes in the tropics, and the recognized role of cloud cover in driving shallow warm water formation linked to coral bleaching. This study aims to address two scientific questions: (1) What are the characteristics of the diurnal cloud and rainfall cycles over coastal and open ocean regions of north–east Queensland? (2) How do the background wind fields interact with local–scale processes to shape these diurnal patterns? Focusing on the Coral Bleaching Season (CBS; January–April), when most CBEs in the GBR occur, we use a multi–year dataset combining high–resolution geostationary satellite observations (Himawari–8), C–band radar data, and BARRA–R2 regional reanalysis. Through this integrated approach, we characterize diurnal cycles of cloud and rainfall, and examine the thermodynamic and dynamical factors that modulate them. Drawing on the observed patterns, we propose plausible mechanisms underlying these interactions, offering a foundation for targeted process studies in future work.

2 Data and Methods

2.1 Observational and Reanalysis Datasets

Cloud diurnal cycles were analyzed using Channel 13 Brightness Temperature (BT) from the Himawari–8 satellite Level 1 atmospheric and cloud property dataset, which covers the Australian region at an hourly temporal and 2 km spatial resolution (Lopez-Bravo et al., 2021a, b). The BT data was regridded for the study domain, spanning 21.5°–14° S and 143°–152° E, encompassing a region of north–east Queensland, the central GBR and the Coral Sea, including the coverage areas of three weather radars (Fig. 1). Diurnal cloud characteristics were analyzed for the January to March period — including small convective clouds observable with the high resolution Advanced Himawari Imager (AHI). A shortened Coral Bleaching Season (CBS) was analyzed due to data availability (Jan–Mar rather than the defined CBS Jan–Apr). Previous studies of the same Level–1 dataset have provided detailed insights on diurnal cycles of convection in the tropical Maritime Continent (Lopez-Bravo et al., 2023a, b).

Rainfall estimates were obtained from Level–2 rain rate retrievals derived from C–band Doppler radar data. This study uses data from the Townsville, Cairns and Willis Island operational weather radars operated by the Australian Bureau of Meteorology, archived on the National Computational Infrastructure (Soderholm et al., 2022). Rain rate estimates have a spatial resolution of 1 km, extending horizontally from the radar site up to a range of 150 km in all directions (360°), with a

https://doi.org/10.5194/egusphere-2026-1019
Preprint. Discussion started: 10 March 2026

temporal resolution between 5–10 min (increasing in frequency towards the end of the analysis period). The analysis focuses on the full CBS (Jan–Apr), for the years when data from for all three radars are available (2012–2022).

Surface wind data from the Australian Bureau of Meteorology's automated weather stations (AWS) in Townsville and Cairns are used to highlight the complex local–scale influences on surface conditions. AWS data was analyzed for the full CBS for the period of 1990 to 2020, with a temporal resolution of 30 min. The location of both stations is shown in Fig. 1, with height above sea level of 4.34 m for Townsville and 2 m for Cairns (with wind measurements 10 m above ground level).

The Australian Bureau of Meteorology Atmospheric high–resolution Regional Reanalysis for Australia (BARRA–R2) was used to provide meteorological context for the radar rainfall and satellite cloud observations. BARRA–R2 covers the Australian region from 1979 to the present, with a horizontal grid resolution of 12 km and a temporal resolution ranging from hourly to monthly; this study focuses on variables at hourly resolution. Full documentation can be found in Su et al. (2022). Previous studies have used the BARRA–R2 reanalysis to examine diurnal cycles of temperature and humidity over northern Australia (May et al., 2022). The higher horizontal resolution of BARRA–R2 compared to global reanalyses enables improved representation of local features such as coastal and topographic circulations, though fine–scale processes (such as convection) remain parametrized. In this study, BARRA–R2 was used primarily for defining the background wind and local environmental conditions through composite analysis, as described in Section 2.2.

2.2 Methods

Large–scale meteorological conditions were characterized using hourly mean 850 hPa wind direction from BARRA–R2 across each radar domain for the full CBS from 2012 to 2022. Wind regimes at 850 hPa were categorized as north–easterly (0°–90°), south–easterly (90°–180°), south–westerly (180°–270°) and north–westerly (270°–360°). This classification was designed to establish a clear northerly–southerly distinction, effectively separating tropical air masses (typically warmer and more humid) from those of mid–latitude origin (typically cooler and drier). Due to the variation in coastline orientation across the radar domains, a simple easterly–westerly division was also adopted to ensure consistency and interpretability in the analysis. Further characterization of meteorological conditions were performed by calculating vertical profiles of equivalent potential temperature (θ_e) using BARRA–R2 temperature and specific humidity over the Townsville, Cairns and Willis Island radar domains for each wind regime. Higher values of θ_e suggest warmer or more moisture–rich conditions, whereas lower values are associated with colder or drier conditions.

Prior to the diurnal analysis, the rain rate data required pre–processing to remove regions with erroneous data caused by the partial radar beam blockage from complex topography around the Townsville and Cairns radar sites. To identify regions with erroneous rain rate data, the climatological mean rain intensity over 2012–2022 was calculated, and a lower threshold was applied to exclude affected data from the diurnal analysis: 0.8 mm h^{-1} for Townsville and 1.2 mm h^{-1} for Cairns. No lower threshold was applied to the Willis Island radar data, as the highest elevation on the island is 20 m above sea level and topographic blockage is absent. However, the Willis Island radar exhibited the highest proportion of missing temporal data — 6.65% of periods analyzed — and also carries greater uncertainty in its rain rate retrievals due to the absence of co–located in situ rain gauges for calibration (Bowden et al., 2024).

https://doi.org/10.5194/egusphere-2026-1019
Preprint. Discussion started: 10 March 2026

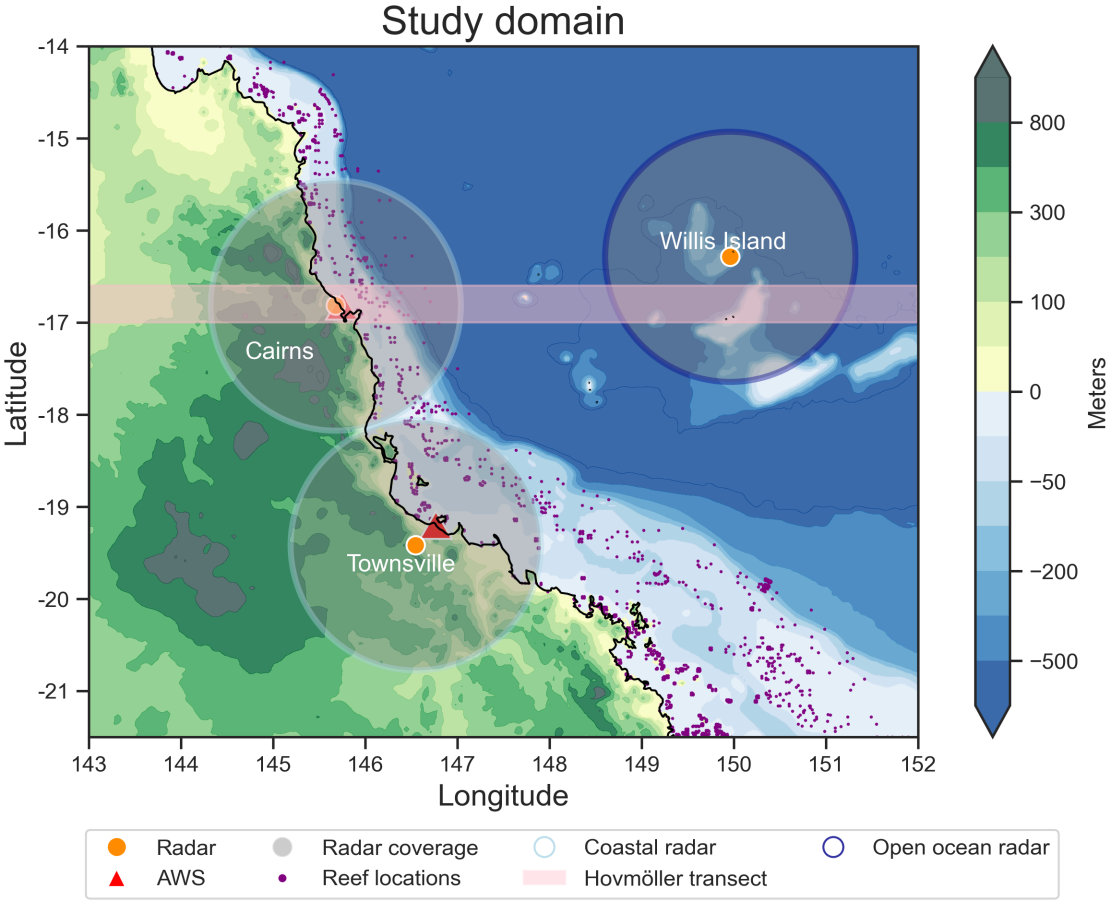

Figure 1. Map of the study domain, including elevation above and below sea level for north–east Queensland produced using the NOAA ETOPO2 dataset. Shown is the complex coastal topography, shallow coastal oceans of the GBR, with reef locations (purple markers), and the deep bathymetry of the open ocean. The three large circles show the spatial coverage of the Townsville, Cairns and Willis Island radars, with orange markers indicating the radar site location. Townsville and Cairns Automated Weather Station (AWS) locations are marked by red triangles. Defined coastal and open ocean regions are indicated by the light blue and navy radar domain colours respectively (the coastline in black divides coastal land and ocean regions). Hovmöller analyses (see 2.2) is conducted over the horizontal transect shaded in pink.

Diurnal cloud and rainfall analyses focused on three distinct regions: coastal land, coastal ocean and open ocean, as indicated in Fig. 1. Coastal land is defined as land areas within the Cairns and Townsville radar domains, while coastal ocean encompasses the oceanic portions of these radar domains. These regions were delineated using land–sea masks derived from the National Oceanic and Atmospheric Administration (NOAA) 2–minute Gridded Global Relief Data (ETOPO2) v2 dataset, which provides high–resolution topography, bathymetry and shoreline information (NOAA National Geophysical Data Center, 2006). In this classification, coastal ocean areas are defined by surface elevation below 0 m ($z < 0$) and coastal land by elevation above 0 m ($z \geq 0$). The open ocean is defined as the area within the Willis Island radar domain. Given that Willis

https://doi.org/10.5194/egusphere-2026-1019
Preprint. Discussion started: 10 March 2026

Island lies about 450 km from the Queensland coastline, and measures only about 500 m in length and 150 m in width, it is considered to have little to no land–surface influences on local convection and rainfall processes.

The diurnal mean hourly values of cloud BT, rain intensity and rainfall frequency across the CBS were computed for each of the three regions — coastal land, coastal ocean and open ocean — under the defined wind regimes. Rain intensity and frequency were calculated using a ±30–minute window around each hour to match the hourly temporal resolution of the cloud BT dataset. Rain intensity calculations include all time periods (i.e. raining and non–raining) to maintain consistency with BT diurnal cycles. An example of satellite–derived channel 13 BT and corresponding radar rain rate retrievals at a single time step over the Cairns radar domain is provided in Fig. 2.

The diurnal evolution of cloud and rainfall was examined through a Hovmöller analysis. A longitudinal transect was chosen which spans the coastal land, coastal ocean and open ocean regions (shown in pink in Fig. 1). This transect crosses both the Cairns and Willis Island radar domains, offering simultaneous data on cloud and rainfall characteristics for coastal land, coastal ocean and open ocean regions. Mean hourly values of BT and rain intensity were calculated for each longitude point along the transect using a narrow latitude range (16.6°–17° S), to minimize radar–induced noise. These data were used to generate Hovmöller diagrams that represent the mean diurnal cycle of each variable and reveal patterns in the spatiotemporal propagation of cloud and rainfall features across the domain.

3 Results

3.1 Background wind regimes

The large–scale wind regimes during the CBS period play a crucial role in shaping local thermodynamic environments and convective behavior. This section examines the characteristics of the four wind regimes (850 hPa winds) defined in Section 2.2. Figure 3a shows the composite 850 hPa winds for each regime at the three study sites, while the monthly frequency distribution is presented in Fig. 3b–d. Additional statistical summaries are provided in Table A1 in Appendix A.

The south–easterly wind regime, representing the trade winds, dominated across all three sites, accounting for 60–70% of the CBS period. At Townsville, south–easterly winds were least frequent in January (about 50%) but increased steadily to nearly 80% by April. Cairns and Willis Island showed a more delayed transition, with relatively stable frequencies in January–February followed by a marked increase in March and April. This north–south contrast may reflect stronger tropical influences at the lower–latitude sites early in the season, and a progressive strengthening of the trade wind belt as the Inter–Tropical Convergence Zone (ITCZ) shifts northward.

The north–easterly wind regime was on average the second most common regime across all three sites during the CBS, occurring 14–24% of the time on a seasonal mean basis. It was most commonly observed in January and February over Townsville (33.7% and 28.3% respectively). Cairns and Willis Island exhibit less month–to–month variation north–easterly frequencies (18.6–20.2%) during the same period of time, with a similar drop–off from March onward (Fig. 3b, c). This regime's seasonal decline coincides with the strengthening south–easterlies, indicating a shift in dominant flow as the tropical influence weakens.

https://doi.org/10.5194/egusphere-2026-1019
Preprint. Discussion started: 10 March 2026

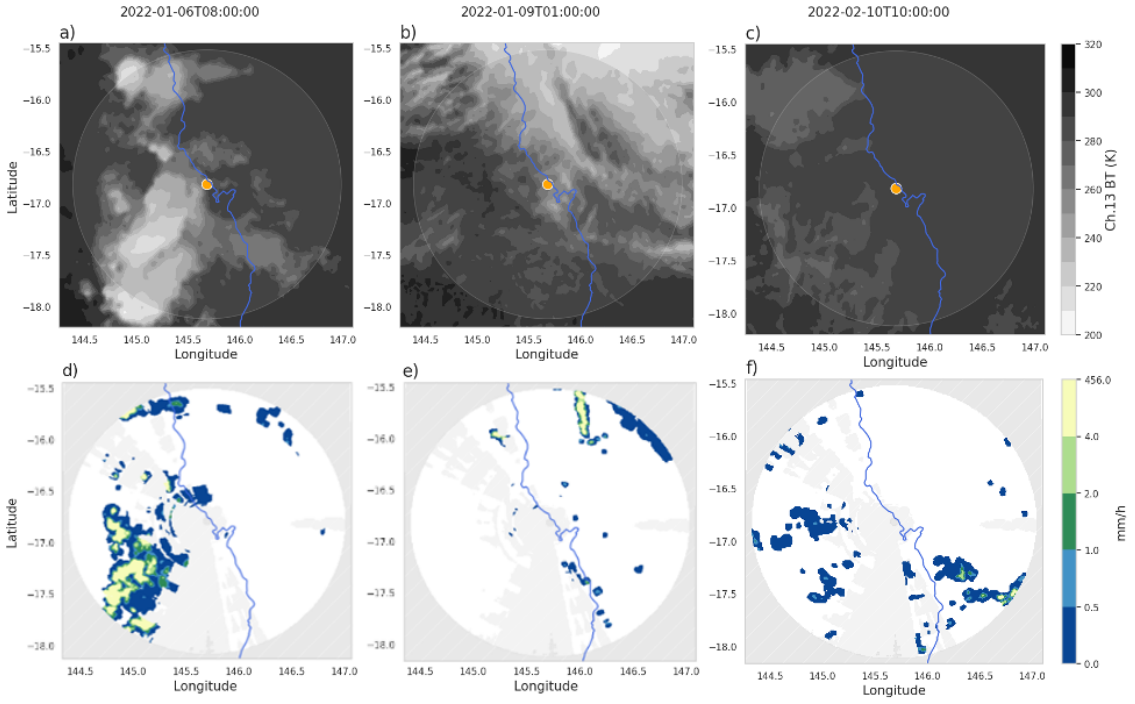

Figure 2. Snapshots of the cloud fields from satellite channel 13 BT and Cairns radar rain rate fields in UTC for: (a,d) 0800 06–01–2022; (b,e) 0100 09–01–2022; and (c,f) 1000 10–02–2022. All plots show the Cairns radar domain, with the Queensland coastline marked in blue (land on left). In (a,b,c) orange markers indicate the Cairns radar site location, with a larger gray circle showing the radar range. Cloud BT is shown in gray–scale shading where white indicates colder BTs, and black indicates warmer BTs. Rain rate in (d,e,f) is shaded in color, with gray hatching indicating regions where no observations are taken (i.e. the corners of the Constant Altitude Plan Position Indicator radar retrieval grid) or masked (due to radar beam blockage).

North–westerly and south–westerly regimes were relatively infrequent, each occurring in 6–12% of CBS periods, with peak frequencies during January–February and a marked decline by April. South–westerlies became especially rare at Willis Island in April (3.5%). While the northwesterly regime is likely associated with transient tropical lows, monsoonal flow, or monsoon burst events (Hung and Yanai, 2004; Wheeler and McBride, 2012), the south–westerly regime is likely more closely linked to the passage of cold fronts driven by deep mid–latitude troughs along the east coast (Kong and Zhao, 2010). The enhanced westerly flow and deep convection typical of north–westerlies are also consistent with active MJO phases influencing northern Australia (Dao et al., 2023).

In summary, south–easterly trades dominate the CBS period, with a clear seasonal transition replacing early–season tropical and cyclonic regimes — which drive the higher frequency of northerlies (Richards et al., 2025). Latitudinal differences suggest stronger tropical influence at Cairns and Willis Island, particularly early in the season, likely modulated by MJO activity, monsoon flows and ITCZ positioning.

https://doi.org/10.5194/egusphere-2026-1019
Preprint. Discussion started: 10 March 2026

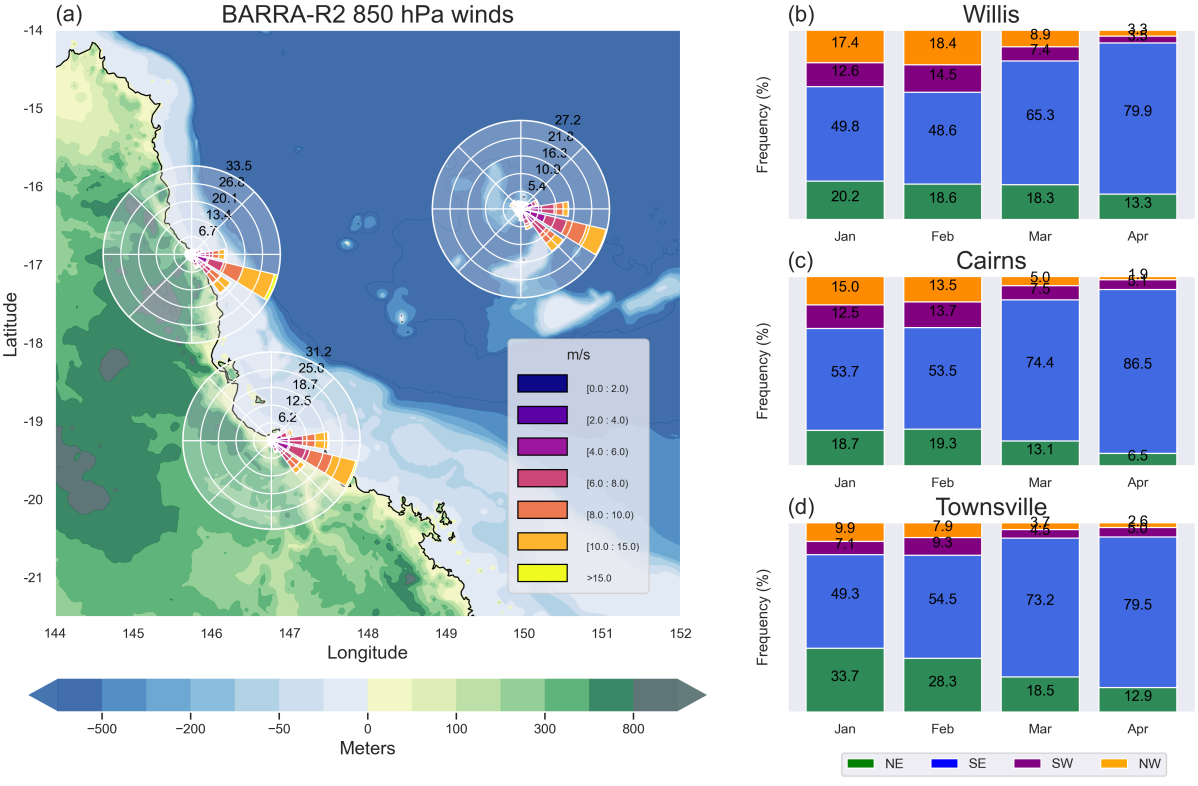

Figure 3. (a) BARRA–R2 850 hPa wind regimes defined in Section 2.2 for the CBS, and (b,c,d) regime frequency each month for Willis Island, Cairns and Townsville. BARRA–R2 850 hPa winds are averaged over each site's radar domain (see Fig. 1) for the CBS over the period 1979–2024.

3.2 Thermodynamic environment

To better understand the convective environments associated with each wind regime, we examine the thermodynamic structure of the atmosphere using vertical profiles of equivalent potential temperature (θ_e) from BARRA–R2. θ_e is a combined measure of temperature and moisture, and it provides a useful indicator of an air parcel's convective potential. Higher values of θ_e typically signify warmer, moister air masses, while lower values suggest drier or cooler air masses. The vertical structure of θ_e also reveals information about boundary layer depth and stability, taking into account latent heat release from condensation of the moisture in the air. The CBS mean and wind–regime–averaged θ_e profiles for the three sites are shown in Fig. 4a, c, e, with anomalies shown in Fig. 4b, d, f.

The four large–scale wind regimes exhibit distinct thermodynamic signatures, as reflected in their θ_e anomaly profiles relative to the seasonal composite mean. The south–easterly regime is characterized by the strongest negative θ_e anomalies throughout the atmospheric column, indicating cooler and drier conditions likely originating from the subtropical Pacific. This regime is also marked by enhanced stability above the 600 hPa inversion (θ_e anomaly increasing with height), strongly

https://doi.org/10.5194/egusphere-2026-1019
Preprint. Discussion started: 10 March 2026

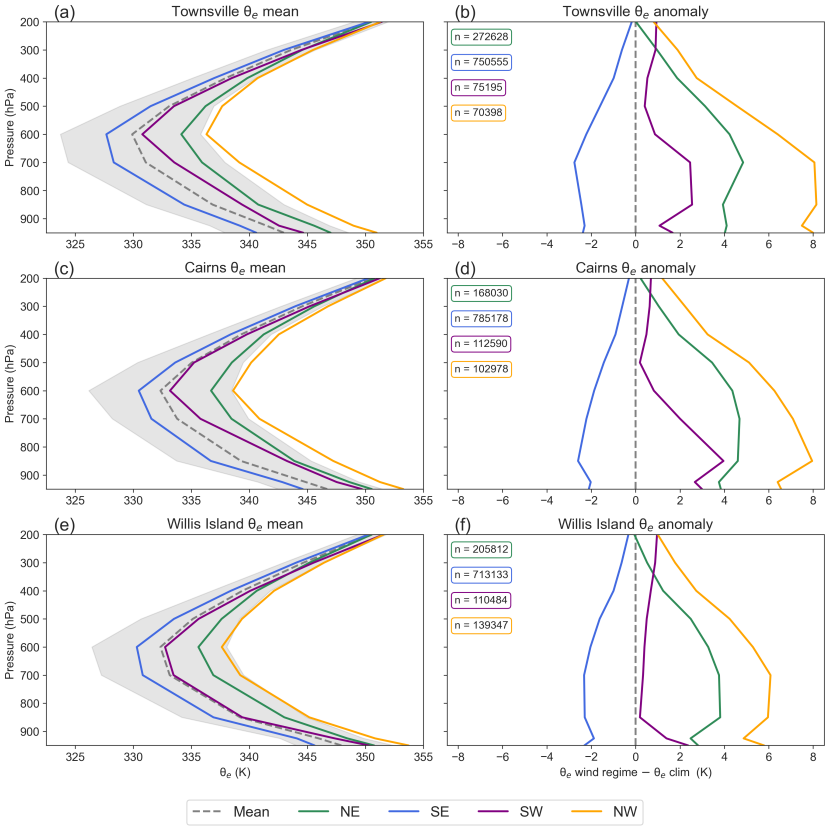

Figure 4. Mean and anomaly θ_e profiles for Townsville (a,b), Cairns (c,d) and Willis Island (e,f) domains under each wind regime (north–easterly: NE, south–easterly: SE, south–westerly: SW, and north–westerly: NW) for the CBS over the period 1979–2024 from BARRA–R2. Sample sizes for each site across all times and pressure levels are provided for each regime. Grey shading indicates the interquartile range of the θ_e profile.

suppressing deep convection. In contrast, the north–easterly regime displays persistent positive θ_e anomalies in the lower and mid–troposphere, reflecting the influence of warm, moist air masses from lower latitudes. However, the relatively weak vertical θ_e gradient below the inversion suggests limited buoyancy and somewhat suppressed convective development despite the elevated total energy. South–westerly regimes reveal a land–ocean contrast: over land, it shows modest positive θ_e anomalies and signs of surface–driven instability, while at Willis Island, θ_e remains closest to the climatological mean, implying minimal thermodynamic departure from baseline maritime conditions. North–westerly regimes exhibit the most pronounced positive θ_e anomalies, particularly in the lower and mid–levels, alongside steep vertical gradients that signal strong instability and high convective potential. These patterns are consistent with monsoonal or tropical intrusions that inject warm, moist, and energetically favorable air into the region. Together, these characteristics highlight how large–scale flow direction modulates

https://doi.org/10.5194/egusphere-2026-1019
Preprint. Discussion started: 10 March 2026

both the source characteristics of air masses and the vertical thermodynamic structure that governs convective potential across the study region.

The diurnal evolution of θ_e (Fig. 5) across the three sites highlights the combined influence of synoptic wind regimes and surface characteristics on the boundary layer structure and convective potential. At the two coastal land sites — Townsville and Cairns — θ_e profiles show stronger diurnal modulation, especially under south–westerly regimes, reflecting land surface heating and boundary layer deepening during the day. Townsville exhibits the most pronounced diurnal growth in θ_e under south–westerly flow, pointing to enhanced surface–driven convection. Cairns shows similar patterns, albeit more subdued, with notable θ_e enhancement below 600 hPa under south–westerly conditions. In contrast, Willis Island shows minimal diurnal variability across all regimes, reflecting the stabilizing influence of the ocean surface. Regime–wise, north–westerly flow at all sites generally brings high θ_e values and weaker stability, favoring convection, while north–easterly flow produces moist but capped profiles with limited diurnal evolution. South–easterly regimes consistently feature the lowest θ_e values and most stable conditions across all sites, indicating suppressed convective potential. Overall, these features underscore the interplay between large–scale flow direction and surface type in shaping diurnal thermodynamic evolution and the likelihood of convective activity.

3.3 Diurnal cloud and rainfall characteristics

Next we examine how these thermodynamic conditions influence the diurnal evolution of cloud and rainfall patterns. Differences in vertical stability and moisture content across wind regimes are expected to influence not only the likelihood of convection but also its timing and intensity throughout the day. The mean diurnal cycles of satellite–derived Brightness Temperature (BT) from channel 13 and radar–derived rainfall frequency and intensity under different wind regimes are presented in Fig. 6. The seasonal mean conditions are provided in the Supplementary Material (Fig. **??**). BT serves as a proxy for cloud height and type — colder BTs indicate higher, deeper clouds often associated with convection, while warmer BTs suggest fewer or lower–level clouds.

North–easterly regime is characterized by relatively colder BTs, and more frequent, intense rainfall than the seasonal mean, especially over land. Cairns, in particular, experiences the strongest diurnal signals among all three sites, with BTs over land warming through the morning (peaking around 12 LT at 277 K) and sharply cooling into evening (250 K by at 19 LT), indicative of deepening convection. Townsville shows a similar warming trend (approximately 1 K per hour) but with more gradual cooling, about half of the rate at Cairns, likely reflecting the reduced influence of orographic uplift and elevated terrain heating compared to Cairns. Rainfall frequency and intensity at both land sites mirror these BT patterns, peaking in the afternoon–evening, especially at Cairns, with moderate amplitudes of 6.25% and 0.34 mm h^{-1}. Notably, peak rainfall precedes the coldest BTs by several hours, suggesting that the coldest BTs likely reflect the expansion of convective anvil clouds following the main rainfall event. Over the coastal oceans, rainfall follows the BT cycles which are present but with weaker amplitudes, with both rainfall peaks and minimum BTs occurring in the evening. Willis Island shows minimal diurnal variation in either field, consistent with weaker surface forcing. Overall, the diurnal variations in cloud and rainfall across these

https://doi.org/10.5194/egusphere-2026-1019
Preprint. Discussion started: 10 March 2026

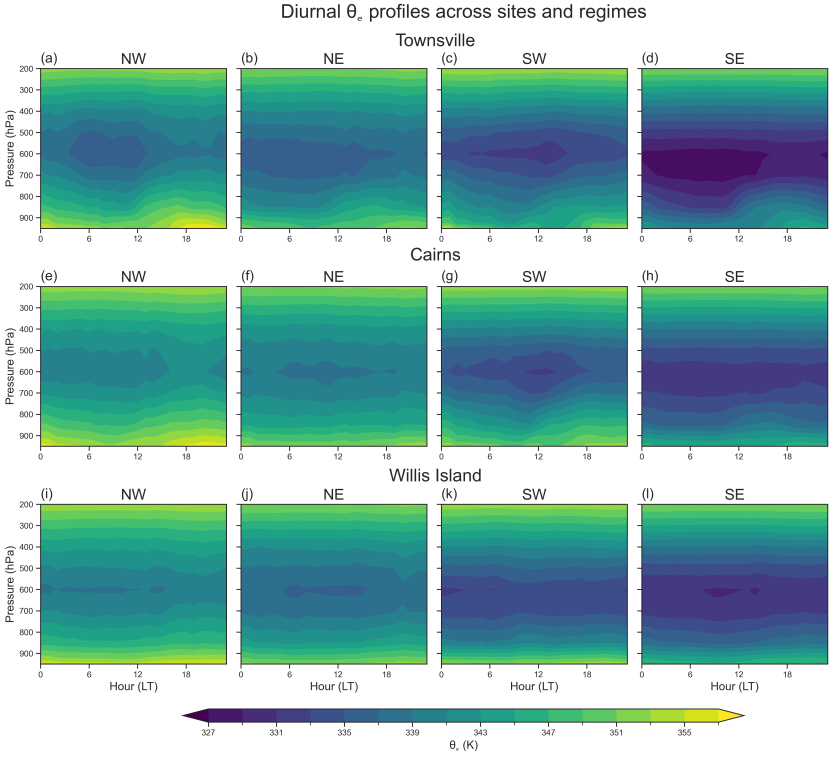

Figure 5. Hourly mean equivalent potential temperature profiles for (a, b, c, d) Townsville, (e, f, g, h) Cairns and (i, j, k, l) Willis Island radar domains under each wind regime (north–westerly: NW, north–easterly: NE, south–westerly: SW, and south–easterly: SE) for the CBS over the period 1979–2024 from BARRA–R2.

sites and the land–ocean contrast align with thermodynamic conditions marked by high total energy but somewhat constrained buoyancy, which limits the potential for deep convective development.

The south–easterly regime, dominated by trade–wind conditions, exhibits the warmest BTs and the lowest rainfall frequencies and intensities across all land regions — with the exception of the south–westerly regime during the day. These patterns suggest shallow, low–topped cumulus clouds and reduced convective activity. Unlike the north–easterly regime, BT and rainfall diurnal cycles over Cairns and Townsville are more synchronized and subdued, though rainfall intensity over Cairns is slightly enhanced in the afternoon — likely due to orographic lifting/elevated heating. Cloud and rainfall variability over the coastal and open ocean remains limited, with minimal diurnal amplitude, consistent with the more stable marine boundary layers and low–level trade wind cumulus. These characteristics are broadly consistent with the thermodynamic constraints described above.

South–westerly regimes display very strong diurnal modulation in both BT and rainfall, suggesting enhanced surface–driven convection. Over Cairns and Townsville, BTs peak around midday 11–13 LT (295 K), indicating minimal cloud cover, and drop sharply in the afternoon. Correspondingly, rainfall frequency and intensity are minimal around midday but increase later

https://doi.org/10.5194/egusphere-2026-1019
Preprint. Discussion started: 10 March 2026

in the day, with maxima in the late afternoon over land and early morning over the coastal ocean. Cairns generally exhibits more rainfall than Townsville, particularly in the afternoon–evening. Oceanic domains show comparable rainfall magnitude across both coastal sites, while Willis Island again shows little diurnal variability, reflecting its open–ocean character. These patterns align with the south–westerly regime fostering deeper, more organized convection through localized surface heating and atmospheric destabilization.

The north–westerly regime is associated with the coldest BTs and the most frequent and intense rainfall, particularly during the peak phase of the diurnal cycles. Over land, convection deepens through the afternoon, accompanied by cooling BTs and increased rainfall. Again, the rate of change in cold BTs lags the increase in rainfall by several hours, likely reflecting the typical progression of convective development: rainfall intensifies during the early to mature stages of convection, while significant BT cooling (marking the development of deep cloud tops) peaks later, during the mature to stratiform transition phase. Notably, the coastal ocean domains show strong diurnal cycles, with daytime (11–14 LT) BT warming and suppressed rainfall, followed by nocturnal intensification. The large amplitudes of cloud and rainfall signals over the coastal ocean highlight the strong diurnal forcing under the north–westerly regime. In contrast, over the open ocean (Willis Island) the cloud BT and rainfall cycle is weak with no clear signals. The north–westerly observed cloud and rainfall characteristics correspond to strong instability from elevated θ_e and steep gradients, fueled by moist north–westerly inflow. Diurnal patterns over land and coastal ocean reflect surface heating and boundary–layer dynamics.

Overall, the diurnal variations in brightness temperature and rainfall are strongly influenced by prevailing wind regimes, which control the depth and intensity of convection through their thermodynamic characteristics. North–westerly flows promote deeper, more intense convection and rainfall, while southeasterly trades favor shallower, weaker cloud systems with limited rainfall. Surface heating and boundary–layer processes drive pronounced diurnal cycles over land and coastal regions, particularly under south–westerlies, but these effects diminish over the open ocean.

3.4 Spatial structure and propagation

Building on the discussion of diurnal BT and rainfall, Hovmöller diagrams were produced to examine evolution over time. Using the method discussed in Section 2.2, Fig. 7 shows BT and rain intensity (averaged across both raining and non–raining periods) under each wind regime defined by the Cairns domain.

Under the north–easterly regime, widespread moderate coastal rainfall persists throughout the day, consistent with a moist environment. BTs over the coastal ocean region remain colder than 273 K throughout the diurnal cycle. The coldest BTs (below 263 K) are observed over land and the adjacent coastal ocean in the evening to early morning. From around 12 LT, BTs below 273 K begin to propagate across coastal areas, both inland and offshore. Inland convection advances westward at speed of 30 m s^{-1}, reaching the western boundary of the study domain, over 300 km from the coastline. Apparent eastward propagation over the domain also occurs at similar speeds, crossing the westward edge of the Willis Island domain, about 300–400 km offshore. However, this offshore signal may reflect a broader open–ocean feature rather than true propagation, since colder BTs can also be seen over the open ocean under other regimes with no clear link to coastal activity. BTs below 263 K first appear over coastal land around 16 LT and then propagate inland at similar speeds and distances. The coldest BTs are typically

https://doi.org/10.5194/egusphere-2026-1019
Preprint. Discussion started: 10 March 2026

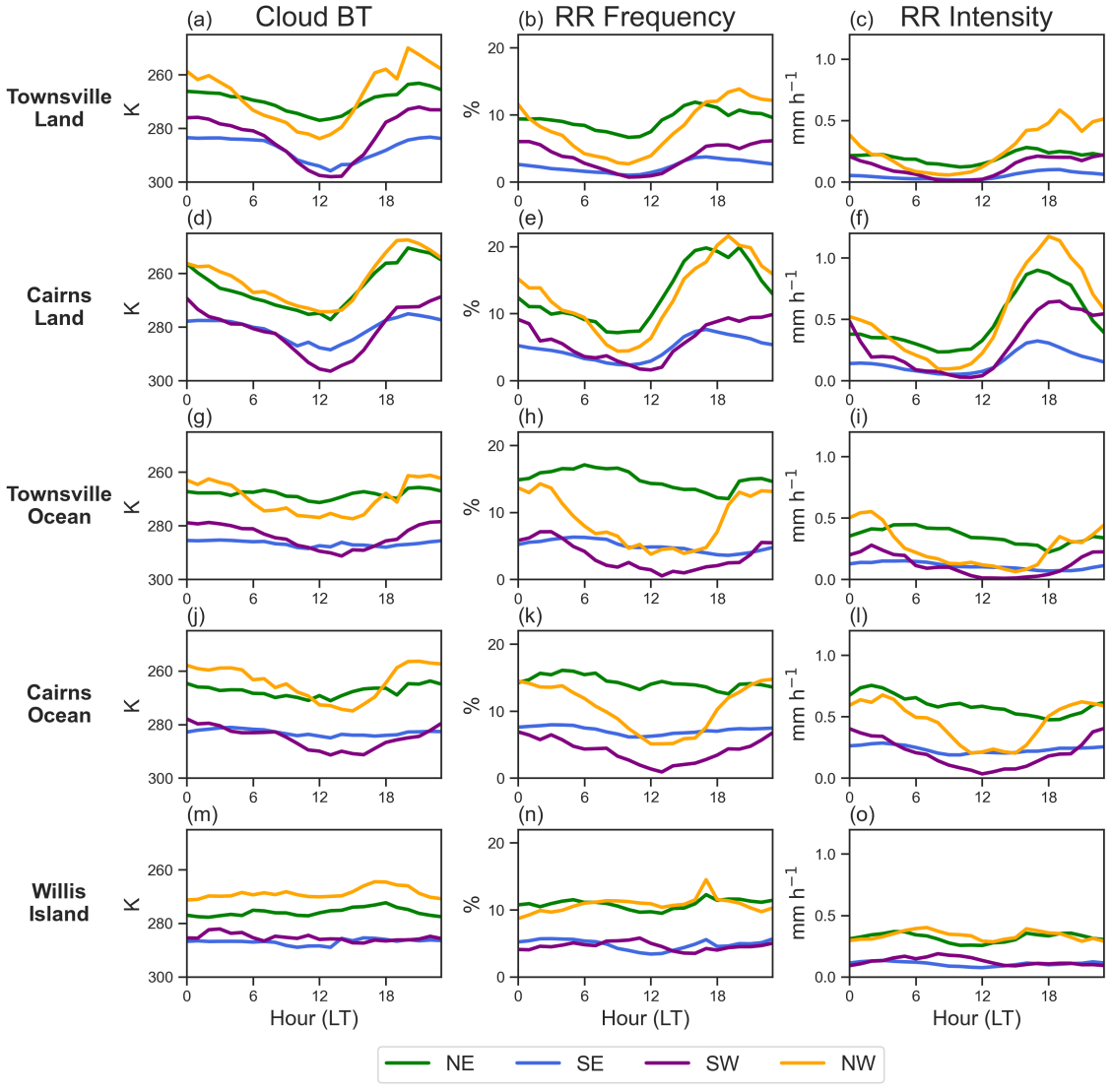

Figure 6. Diurnal cycle hourly means of Himawari–8 satellite channel 13 BT, radar retrieved rainfall frequency and intensity calculated over the CBS for each wind regime and site. Each row (a, b, c) shows the corresponding BT, rainfall frequency and intensity for each site– with Townsville and Cairns separated into land and ocean domains, associated with their radar coverage. The BT y–axis is inverted, so that peaks in the diurnal cycle indicate colder BTs. Rain intensity is calculated for all periods of valid data (not just raining periods).

found on the leeward side of the mountain ranges between 18–22 LT, traveling westward — suggesting convection enhanced by mountain effects that produce strong thunderstorms propagating westward into the evening.

Under south–easterly regimes, light–to–moderate coastal rainfall is again present but confined to a more limited area. Cold BTs start propagating inland from the coast by 13 LT, penetrating more than 200 km inland at speeds of 12–15 m s^{-1}, with

https://doi.org/10.5194/egusphere-2026-1019
Preprint. Discussion started: 10 March 2026

the coldest BTs emerging about 250 km from the coast in the late evening between 22–01 LT, suggesting storm enhancement during inland propagation. Rainfall follows a similar westward propagation, though slightly slower (10–15 m s^{-1}), and generally tracks the BT contours. Notably, a spike in afternoon rain intensity is observed over elevated terrain, which may reflect orographic enhancement rather than a propagating disturbance, though potential radar artefacts cannot be ruled out. Over the coastal ocean, convection is less clearly defined, and no consistent signal of offshore propagation is observed.

For south–westerly regimes, coastal rainfall exhibits a pronounced diurnal cycle, with little to no rainfall occurring from early morning through to the afternoon. Hovmöller analysis indicates BTs below 273 K forming over land, particularly on the windward side of the topography. This convection then propagates both inland and offshore, with the coldest BTs occurring between 20–23 LT over land. Relatively cooler bands of convection can be seen moving offshore reaching distances of approximately 200 km, associated with light rainfall. In general, rainfall contours track closely with cloud BTs, although peak rainfall (orange and red contours) often occurs prior to the appearance of the coldest BTs — again suggesting these may correspond to high–level anvil clouds decoupled from topographic influence. This regime is also the only one to show rainfall possibly aligned with BT propagation over Willis Island (03–09 LT), although the low rainfall frequency means there is considerable uncertainty.

Under north–westerly regime, BTs below 263 K develop by 17 LT over coastal land, especially on the windward side of the topography. Nighttime propagation of convection is evident over the coastal and open oceans, with BTs below 273 K reaching 200–300 km offshore, and extending to the eastern edge of the study domain. Inland propagation is less well defined. The coldest BTs are largely confined to near–coastal waters (within 100 km of the coastline) and are associated with rainfall moving at slower speeds (2–5 m s^{-1}). In contrast, warmer BTs propagate farther offshore more rapidly, at speeds of 12–15 m s^{-1}). In this regime, the coldest BTs correspond closely with the most intense rainfall.

The spatial patterns and propagation characteristics of the BTs and rainfall suggest that land–sea breeze circulations play a variable but important role in shaping the diurnal development of convection over north–east Queensland, depending on the prevailing wind regime. Figure 8 presents wind roses at 07:00 and 15:00 local time, alongside the diurnal evolution of hourly average wind speed and direction at Cairns and Townsville stations. While a classic wind reversal pattern is not observed (likely due to the region's complex coastal geometry and orographic influences), distinct afternoon landward winds indicative of sea–breeze influence are observed at both stations. Similarly, evening seaward winds consistent with land–breeze activity are also evident, supporting the presence of thermally driven circulations despite terrain–induced variability.

Further detail on the variable influence of land–sea breeze circulations can be seen in the contrasting diurnal convection patterns observed across different wind regimes at Cairns (Supplementary Fig. **??**). Afternoon landward winds are evident across all regimes, though with varying strength, which is a reflection of the modulating effect of background winds and possibly the topographic flows. This variation helps explain the differing speeds and inland reach of the convective propagation seen in Fig. 7, where convection initiates near the coast in the early afternoon and moves inland at speeds characteristic of sea–breeze dynamics. In contrast, seaward winds are most pronounced under the two westerly regimes, aligning with the offshore–propagating convection that peaks in the evening shown in Fig. **??**. This suggests a potential role for nocturnal

https://doi.org/10.5194/egusphere-2026-1019
Preprint. Discussion started: 10 March 2026

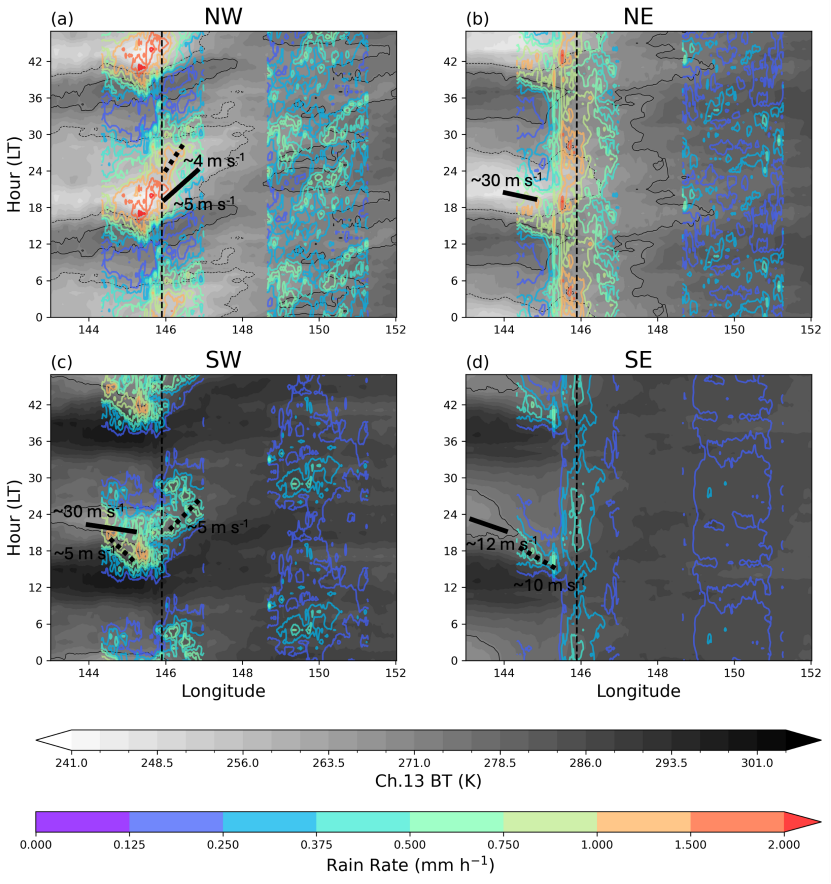

Figure 7. Hovmöller diagram of mean daily cloud BT and rain intensity (including non–raining periods) for the longitudinal transect shown in Fig. 1 under each regime, with rainfall data from the Cairns (left colored contour column) and Willis Island radars (right colored contour column in each plot). The vertical black dashed line marks the coastline (land on left), the solid black contour lines indicate 273 K BT, and dashed black contour lines indicate 263 K BT. Estimates of inland and offshore convection and rainfall propagation are indicated on the plots through solid black and dashed black lines respectively. The y axis (in Local Time; LT) is repeated to show clear propagation of cloud BT and rainfall between the evening and morning.

land breezes in triggering marine convection, though the extent of offshore propagation also depends on ambient moisture availability and background wind strength, which influence the distances over which colder BTs are observed.

4 Discussion

Our analysis reveals distinct diurnal patterns of convection and rainfall across the Greater GBR region, shaped by background wind regimes, geographic features, and atmospheric conditions. Consistent with prior tropical studies, the coldest cloud tops — indicative of deep convection — are primarily observed over land in the evening, coinciding with the timing of upslope

https://doi.org/10.5194/egusphere-2026-1019
Preprint. Discussion started: 10 March 2026

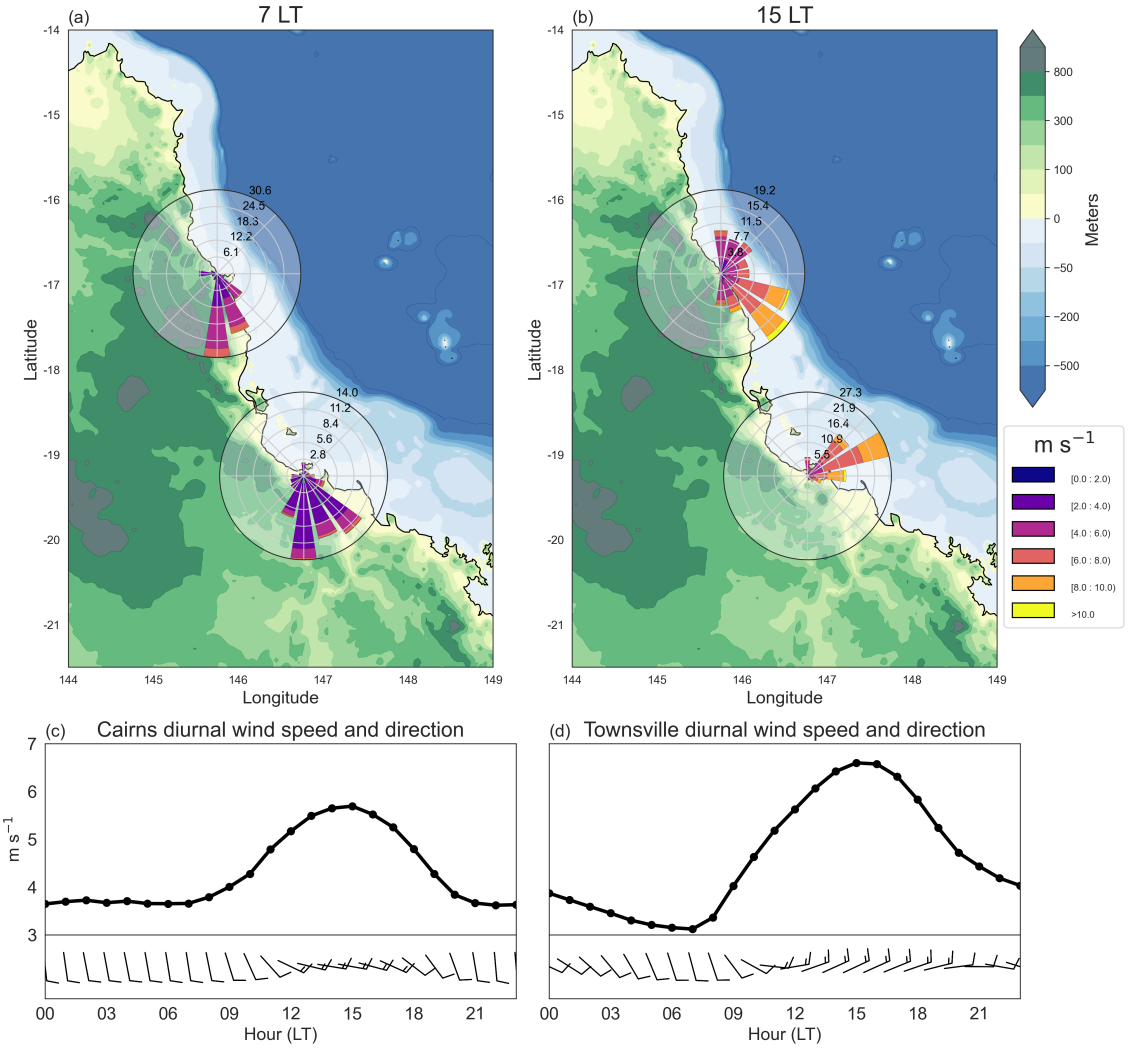

Figure 8. (a,b) Cairns and Townsville AWS surface winds. Wind roses show the surface wind frequency and magnitude at 07 and 15 LT. (c,d) show hourly averaged wind speed and direction (wind barbs) for each station.

winds from daytime heating and sea–breeze convergence. In contrast, convection over the adjacent ocean peaks later, typically overnight to early morning, propagating offshore at speeds consistent with density currents near the coast and gravity waves further offshore. Notably, the influence of land–sea breeze circulations varies across different background wind regimes, modulating the extent, timing, and propagation of convection.

Figure 9 provides a conceptual summary of the contrasting diurnal cycles of cloud and rainfall, along with the hypothetical mechanisms of convection initiation and propagation. The schematic spans five key time periods — early morning, midday, late afternoon, evening, and nighttime — and outlines the general evolution of convection and rainfall across the three sites.

https://doi.org/10.5194/egusphere-2026-1019
Preprint. Discussion started: 10 March 2026

While some elements are necessarily speculative, given the limitations of observations alone, the diagrams synthesize evidence presented in this study and highlight key processes that warrant further investigation in future work.

Under the southeasterly regime, weak large–scale forcing and minimal atmospheric instability limit the development of deep convection. As a result, precipitation is dominated by shallow trade wind cumulus producing light, widespread rainfall. Coastal enhancement is persistent, driven by the combined effects of sea breeze convergence and orographic uplift. Diurnal variability is weak, with rainfall occurring sporadically throughout the day.

In the northeasterly regime, warm, humid air masses advected from lower latitudes contribute to elevated equivalent potential temperature. However, despite the abundant moisture, relatively weak instability and limited buoyancy inhibit the formation of deep convection. Precipitation primarily consists of light to moderate coastal rainfall, with inland propagation driven by the diurnal cycle through combined effects of sea breeze circulations and orographic lifting, and offshore propagation likely influenced by gravity wave activity. North–easterly regimes show the largest inland propagation of deep convection, reaching the up wind (western) side of the coastal mountain ranges. The offshore signal, however, is partially obscured by the widespread moisture associated with this regime.

The southwesterly regime promotes deeper and more organized convection, primarily driven by strong localized surface heating and enhanced atmospheric destabilization. This occurs despite the relatively moderate equivalent potential temperature associated with the cooler air masses linked to passing mid–latitude systems. Pronounced diurnal cycles of cloud and rainfall are observed over both coastal land and adjacent ocean, with the sunniest conditions typically occurring from early morning fostering surface heating that initiates afternoon convection.

The northwesterly regime is characterized by the most intense convection, supported by the highest levels of equivalent potential temperature. It exhibits the strongest diurnal variability and produces the heaviest rainfall among the four regimes. Intense precipitation occurs over both coastal land and adjacent ocean, while widespread, persistent moderate rainfall extends across the open ocean. Although inland propagation is less clearly defined, pronounced offshore propagation is evident and appears consistent with a transition from density current outflow to gravity wave–driven processes.

Together, these four regimes highlight the diverse atmospheric conditions influencing clouds and sub–daily rainfall along the Queensland coast. The contrasting roles of large–scale moisture availability, thermodynamic instability, and local forcing mechanisms—such as sea breeze circulations and orographic effects — shape not only the intensity and spatial distribution of clouds and rainfall, but also its diurnal variability.

5 Conclusions

This study characterizes cloud and rainfall diurnal cycles over north–east Queensland during the coral bleaching season, offering a foundation for understanding links between clouds, rainfall, local processes, and surface energy in this climate–sensitive region. Using Himawari–8 data, C–band radar, and BARRA–R2 reanalysis, a multi–year analysis is conducted across coastal land, coastal ocean, and open ocean zones. Key findings are summarized below:

https://doi.org/10.5194/egusphere-2026-1019
Preprint. Discussion started: 10 March 2026

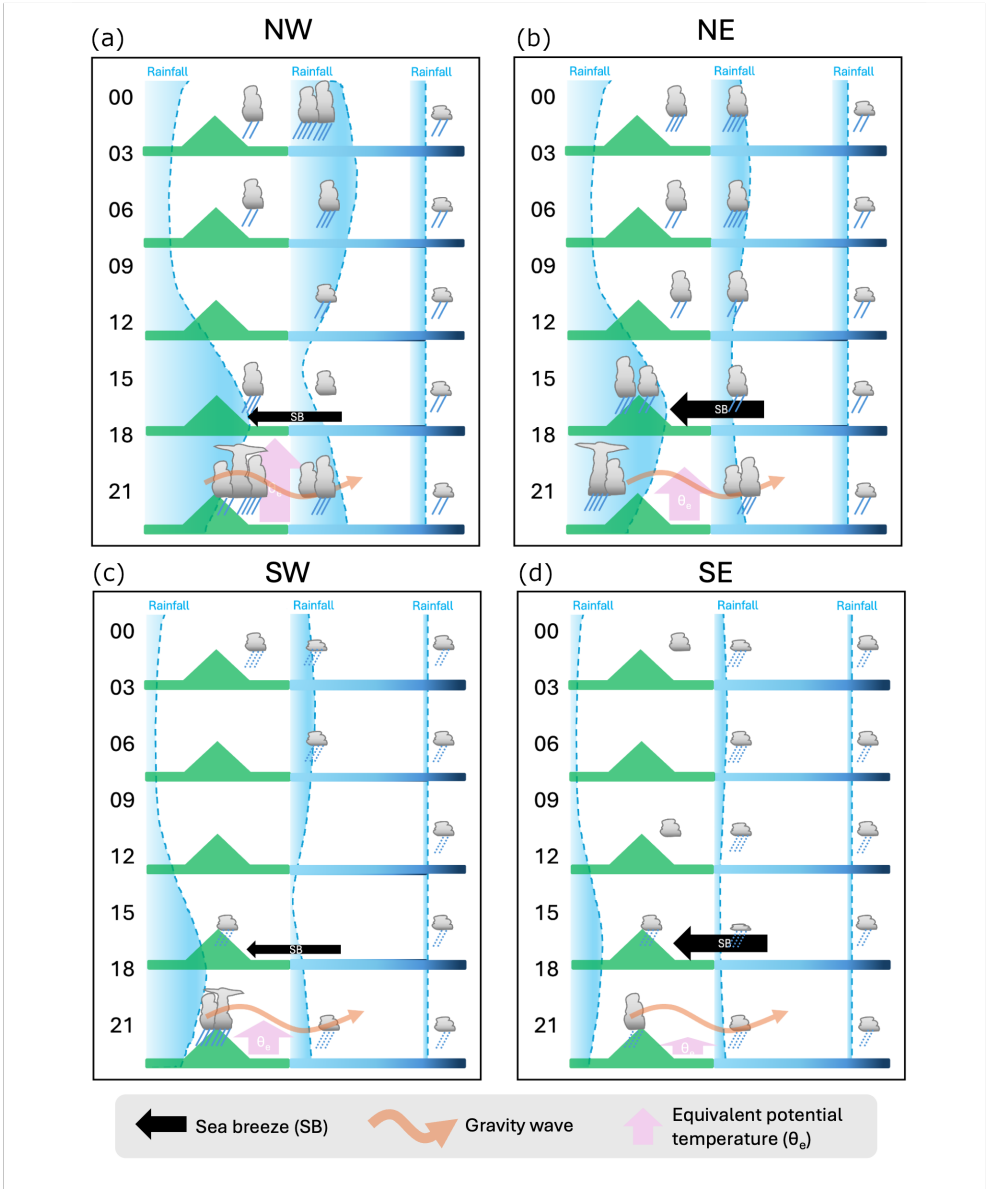

Figure 9. Hypothesized mechanisms for each wind regime (a,b,c,d) cloud BT and rainfall observations. Each panel shows time (Local Time) along the left column, corresponding to mean rainfall changes throughout the day (blue shading). Five distinct stages are shown, with land and topographical features on the left (a general feature of the north–east Queensland coastline), the coastal ocean in the center, and the open ocean on the right. Upward pink arrows indicate the relative size of peak equivalent potential temperatures for each wind regime. The afternoon land sea breeze is shown by black arrows with relative maximum wind speeds indicated by arrow size (see supplementary Fig. **??**). Orange oscillating arrows indicate the nighttime offshore propagation of convection induced by gravity waves.

https://doi.org/10.5194/egusphere-2026-1019
Preprint. Discussion started: 10 March 2026

- Background wind regimes significantly modulate diurnal cloud and rainfall cycles by modulating thermodynamic structure and convective dynamics.
- Strongest diurnal cycles occur under westerly regimes over coastal land, with cloud and rainfall variability significantly reduced over the coastal ocean and minimal over the open ocean.
- The southeasterly regime tends to support shallower and weaker convective systems, resulting in reduced cloud development, limited rainfall and little diurnal variability.
- Cloud and rainfall diurnal cycles are out of phase between land and ocean, with peak cloudiness and rainfall occurring in the evening over land and early morning over the ocean.
- Rainfall peaks precede coldest cloud tops over land, suggesting colder cloud tops often reflect anvil cloud remnants rather than active convective cores.
- Latitudinal and topographic influences are substantial, where Cairns experiences more frequent and intense convection than Townsville.
- Convection propagates more quickly inland but more slowly offshore, highlighting the contrasting dynamics across the region.
- Land–sea breeze circulations and coastal winds exert a variable influence on the spatial patterns and propagation of convection, modulated by ambient moisture availability and background wind strength.

The distinct diurnal patterns of clouds and rainfall identified in this study under different background wind regimes have important implications for the understanding and anticipating coral bleaching risk across the GBR. In particular, the timing and spatial distribution of clouds and rainfall influence the sea surface energy balance and solar radiation exposure, both of which are key drivers of thermal stress on coral reefs. Under westerly wind regimes, clear skies and stronger daytime heating over the coastal zone followed by intense inland convection and reduced cloudiness over the adjacent reef waters may lead to increased SSTs and higher shortwave radiation loads, elevating bleaching risk during heatwaves. Conversely, under easterly regimes, more persistent but less intense cloud cover and rainfall over the coastal ocean may help moderate daytime warming and limit radiation extremes, offering partial thermal protection. Additionally, the offshore propagation of rainfall and cloud anvils during the night may play a role in delaying nighttime cooling or maintaining elevated humidity, further modulating the reef's thermal balance. While our study did not explicitly examine sensible and latent heat fluxes, these processes are likely modulated by the observed wind regimes and atmospheric structure, and may further influence SST variability. Together, these findings highlight the importance of incorporating diurnally evolving mesoscale weather processes, especially those linked to background wind regimes and coastal convection, into assessments and forecasts of coral bleaching risk across the GBR.

https://doi.org/10.5194/egusphere-2026-1019
Preprint. Discussion started: 10 March 2026

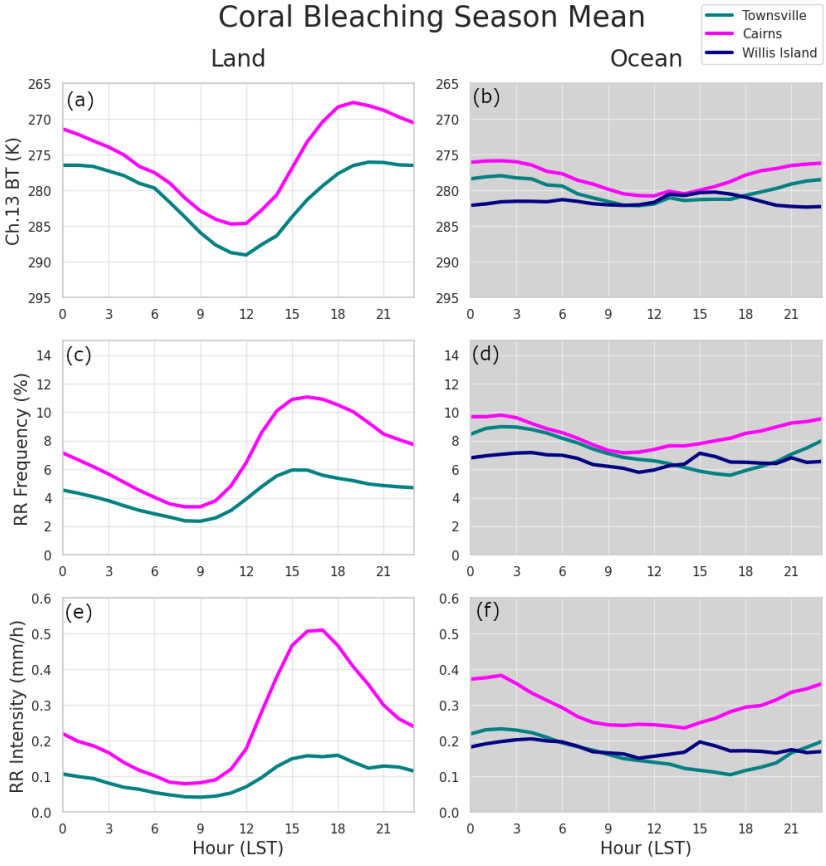

Figure A1. Diurnal cycle plots of (a,b) Himawari–8 satellite channel 13 BT, (c,d) radar retrieved rain rate frequency and (e,f) rate rate intensity calculated from hourly means over the CBS. The cloud BT axis is inverted, so that peaks in the diurnal cycle indicate colder BTs. Townsville (green), Cairns (pink) and Willis Island (blue) diurnal cycles are shown. The subplots in the left column show the cycles of the cloud proxy and rain rate variables for the coastal land, whereas the right column show Townsville and Cairns coastal oceans and the Willis Island open ocean region. Rain rate intensity is calculated for all periods of valid data (not just raining periods).

Code and data availability. The code for this project is hosted on GitHub: https://github.com/alanah-chapman/diurnal-cylces-of-clouds-and-rainfall-over-NE-QLD-during-CBSGitHub. Data from the Level 1 Himawari–8 dataset (Lopez-Bravo et al., 2021a) is available at NCI. The Level 2 Australian Operational Weather Radar dataset (Soderholm et al., 2022) is available at NCI. BARRA–R2 regional reanalysis data (Su et al., 2022) is found on NCI Gadi.

Appendix A

A1

https://doi.org/10.5194/egusphere-2026-1019
Preprint. Discussion started: 10 March 2026

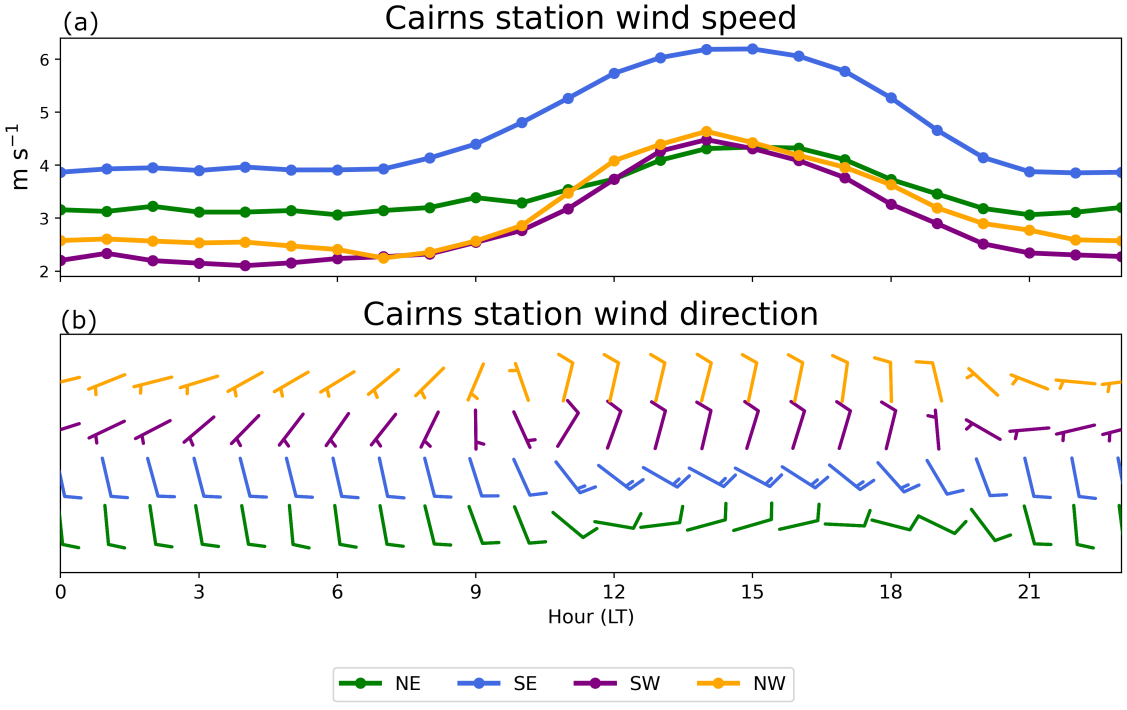

Figure A2. (a) Cairns station surface wind speeds and (b) wind direction (wind barbs) over the full CBS under each wind regime for the period 1990–2020.

https://doi.org/10.5194/egusphere-2026-1019
Preprint. Discussion started: 10 March 2026

Table A1. Statistics on the 850 hPa winds averaged across each radar domain site for the four wind regimes. Note that sample sizes (N) shows the percentage of time periods under each regime for each site. These values were calculated for the CBS from BARRA–R2 wind fields between 1979–2023.

	Mean ($m\ s^{-1}$)	Median ($m\ s^{-1}$)	Maximum ($m\ s^{-1}$)	Minimum ($m\ s^{-1}$)	Standard Deviation ($m\ s^{-1}$)	N (%)
NE Regimes						
Townsville	6.37	6.02	38.57	0.07	3.35	23.3
Cairns	5.33	4.88	20.07	0.07	2.96	14.4
Willis Island	5.35	4.90	34.94	0.08	3.07	17.6
SE Regimes						
Townsville	7.83	7.73	40.05	0.07	3.26	64.2
Cairns	8.28	8.25	27.81	0.06	3.56	67.2
Willis Island	7.35	7.22	33.56	0.01	3.21	61
SW Regimes						
Townsville	4.42	3.97	22.21	0.03	2.68	6.4
Cairns	4.31	3.80	27.89	0.08	2.69	9.6
Willis Island	5.26	4.57	30.27	0.01	3.40	9.5
NW Regimes						
Townsville	4.68	3.93	21.56	0.08	3.26	6
Cairns	5.68	4.86	26.65	0.04	3.78	8.8
Willis Island	6.42	5.51	30.52	0.02	4.31	11.9

https://doi.org/10.5194/egusphere-2026-1019
Preprint. Discussion started: 10 March 2026

Author contributions. AC performed data analyses and contributed to writing the manuscript. YH contributed to project conception, results interpretation, and manuscript writing. CV contributed to results interpretation and research direction.

Competing interests. The authors declare that they have no conflict of interest.

Acknowledgements. The authors would like to acknowledge the Traditional Owners of the Great Barrier Reef. This research was undertaken with the assistance of resources from the National Computational Infrastructure (NCI Australia), an NCRIS enabled capability supported by the Australian Government.

Financial support.

This research is supported by the ARC Centre of Excellence for Climate Extremes (grant no. CE170100023) and the ARC Centre of Excellence for the Weather of the 21st Century (grant no. CE230100012). Yi Huang and Claire Vincent are further supported by an Australian Research Council Discovery Grant (grant no. DP230100639).

https://doi.org/10.5194/egusphere-2026-1019
Preprint. Discussion started: 10 March 2026

References

Birch, C. E., Webster, S., Peatman, S. C., Parker, D. J., Matthews, A. J., Li, Y., and Hassim, M. E. E.: Scale Interactions between the MJO and the Western Maritime Continent, Journal of Climate, 29, 2471–2492, https://doi.org/10.1175/JCLI-D-15-0557.1, 2016.

Bowden, A. J., Jakob, C., and Soderholm, J.: Identification of Rainfall Events and Heavy Rainfall Events From Radar Measurements in Southeastern Australia, Journal of Geophysical Research: Atmospheres, 129, e2023JD039 253, https://doi.org/10.1029/2023JD039253, 2024.

Dao, T. L., Vincent, C. L., and Lane, T. P.: Multiscale Influences on Rainfall in Northeast Australia, 36, 5989–6006, https://doi.org/10.1175/JCLI-D-22-0835.1, 2023.

Hassim, M. E. E., Lane, T. P., and Grabowski, W. W.: The diurnal cycle of rainfall over New Guinea in convection-permitting WRF simulations, Atmospheric Chemistry and Physics, 16, 161–175, https://doi.org/10.5194/acp-16-161-2016, 2016.

Huang, Z., Feng, M., Dalton, S. J., and Carroll, A. G.: Marine heatwaves in the Great Barrier Reef and Coral Sea: their mechanisms and impacts on shallow and mesophotic coral ecosystems, Science of The Total Environment, 908, 168 063, https://doi.org/10.1016/j.scitotenv.2023.168063, 2024.

Hung, C. and Yanai, M.: Factors contributing to the onset of the Australian summer monsoon, 130, 739–758, https://doi.org/10.1256/qj.02.191, 2004.

Kong, Q. and Zhao, S.: Heavy rainfall caused by interactions between monsoon depression and middle-latitude systems in Australia: a case study, 106, 205–226, https://doi.org/10.1007/s00703-010-0060-5, 2010.

Lopez-Bravo, C., Vincent, C. L., and Huang, Y.: Himawari-8 GeoCat 1.0.3 Australian Domain Level 2 v1.0, https://geonetwork.nci.org.au/geonetwork/srv/eng/catalog.search#/metadata/f7783_3730_7872_1101, 2021a.

Lopez-Bravo, C., Vincent, C. L., and Huang, Y.: Himawari-8 GeoCat 1.0.3 Australian Domain Level 1 v1.0, https://geonetwork.nci.org.au/geonetwork/srv/eng/catalog.search#/metadata/f7882_5837_8565_1103, 2021b.

Lopez-Bravo, C., Vincent, C. L., Huang, Y., and Lane, T. P.: A Case Study of a West Sumatra Squall Line Using Satellite Observations, Monthly Weather Review, 151, 523–543, https://doi.org/10.1175/MWR-D-21-0194.1, 2023a.

Lopez-Bravo, C., Vincent, C. L., Huang, Y., and Lane, T. P.: The Diurnal Cycle of Rainfall and Deep Convective Clouds Around Sumatra and the Associated MJO-Induced Variability During Austral Summer in Himawari-8, Journal of Geophysical Research: Atmospheres, 128, e2023JD039 132, https://doi.org/10.1029/2023JD039132, 2023b.

Love, B. S., Matthews, A. J., and Lister, G. M. S.: The diurnal cycle of precipitation over the Maritime Continent in a high-resolution atmospheric model: Diurnal Cycle Over the Maritime Continent, Quarterly Journal of the Royal Meteorological Society, 137, 934–947, https://doi.org/10.1002/qj.809, 2011.

Mapes, B. E., Warner, T. T., and Xu, M.: Diurnal Patterns of Rainfall in Northwestern South America. Part III: Diurnal Gravity Waves and Nocturnal Convection Offshore, Monthly Weather Review, 131, 830–844, https://doi.org/10.1175/1520-0493(2003)131<0830:DPORIN>2.0.CO;2, 2003.

Masson, S., Terray, P., Madec, G., Luo, J.-J., Yamagata, T., and Takahashi, K.: Impact of intra-daily SST variability on ENSO characteristics in a coupled model, 39, 681–707, https://doi.org/10.1007/s00382-011-1247-2, 2012.

May, P. T., Long, C. N., and Protat, A.: The Diurnal Cycle of the Boundary Layer, Convection, Clouds, and Surface Radiation in a Coastal Monsoon Environment (Darwin, Australia), Journal of Climate, 25, 5309–5326, https://doi.org/10.1175/JCLI-D-11-00538.1, 2012.

https://doi.org/10.5194/egusphere-2026-1019
Preprint. Discussion started: 10 March 2026

May, P. T., Trewin, B., Nairn, J. R., Ostendorf, B., Su, C.-H., and Moise, A.: Diurnal and Seasonal Variability of Near-Surface Temperature and Humidity in the Maritime Continent, 61, 1819–1834, https://doi.org/10.1175/JAMC-D-22-0032.1, 2022.

McGowan, H. and Theobald, A.: Atypical weather patterns cause coral bleaching on the Great Barrier Reef, Australia during the 2021–2022 La Niña, Scientific Reports, 13, 6397, https://doi.org/10.1038/s41598-023-33613-1, 2023.

McGowan, H., Sturman, A. P., MacKellar, M. C., Wiebe, A. H., and Neil, D. T.: Measurements of the local energy balance over a coral reef flat, Heron Island, southern Great Barrier Reef, Australia, Journal of Geophysical Research: Atmospheres, 115, https://doi.org/10.1029/2010JD014218, 2010.

Mori, S., Jun-Ichi, H., Tauhid, Y. I., Yamanaka, M. D., Okamoto, N., Murata, F., Sakurai, N., Hashiguchi, H., and Sribimawati, T.: Diurnal Land–Sea Rainfall Peak Migration over Sumatera Island, Indonesian Maritime Continent, Observed by TRMM Satellite and Intensive Rawinsonde Soundings, Monthly Weather Review, 132, 2021–2039, https://doi.org/10.1175/1520-0493(2004)132<2021:DLRPMO>2.0.CO;2, 2004.

Neale, R. and Slingo, J.: The Maritime Continent and Its Role in the Global Climate: A GCM Study, Journal of Climate, 16, 834–848, https://doi.org/10.1175/1520-0442(2003)016<0834:TMCAIR>2.0.CO;2, 2003.

NOAA National Geophysical Data Center: 2-minute Gridded Global Relief Data (ETOPO2) v2, https://doi.org/10.7289/V5J1012Q, 2006.

Peatman, S. C., Birch, C. E., Schwendike, J., Marsham, J. H., Dearden, C., Webster, S., Neely, R. R., and Matthews, A. J.: The Role of Density Currents and Gravity Waves in the Offshore Propagation of Convection over Sumatra, Monthly Weather Review, 151, 1757–1777, https://doi.org/10.1175/MWR-D-22-0322.1, 2023.

Rauniyar, S. P. and Walsh, K. J. E.: Scale Interaction of the Diurnal Cycle of Rainfall over the Maritime Continent and Australia: Influence of the MJO, Journal of Climate, 24, 325–348, https://doi.org/10.1175/2010JCLI3673.1, 2011.

Richards, L. S., Siems, S. T., Huang, Y., Zhao, W., Harrison, D. P., Manton, M. J., and Reeder, M. J.: The Meteorological Drivers of Mass Coral Bleaching on the Central Great Barrier Reef during the 2022 La Niña, Scientific Reports, 14, 23 867, https://doi.org/10.1038/s41598-024-74181-2, 2024.

Richards, L. S., Siems, S. T., Huang, Y., Harrison, D. P., and Zhao, W.: Trade wind regimes during the Great Barrier Reef coral bleaching season, https://doi.org/10.5194/egusphere-2025-3639, 2025.

Slingo, P. Inness, R. Neale, S. Woolnough, and G. Yang: Scale interactions on diurnal toseasonal timescales and their relevanceto model systematic errors, 46, https://doi.org/10.4401/ag-3383, 2003.

Soderholm, J., Louf, V., Brook, J., Protat, A., and Warren, R.: Australian Operational Weather Radar Level 2 Dataset, https://geonetwork.nci.org.au/geonetwork/srv/eng/catalog.search#/metadata/f8188_7912_6774_5057, 2022.

Su, C.-H., Dharssi, I., Le Marshall, J., Le, T., Rennie, S., Smith, A., Stassen, C., Steinle, P., Torrance, J., and Wang, C.: BARRA2: development of the next-generation Australian regional atmospheric reanalysis, 2022.

Vincent, C. L. and Huang, Y.: Meso- and microscale response to variation in cloudiness at three forested sites in the Maritime Continent, Quarterly Journal of the Royal Meteorological Society, 148, 418–433, https://doi.org/10.1002/qj.4212, 2022.

Vincent, C. L. and Lane, T. P.: Evolution of the Diurnal Precipitation Cycle with the Passage of a Madden–Julian Oscillation Event through the Maritime Continent, Monthly Weather Review, 144, https://doi.org/10.1175/MWR-D-15-0326.1, 2016.

Wheeler, M. C. and McBride, J. L.: Australasian Monsoon, in: Intraseasonal Variability in the Atmosphere-Ocean Climate System, pp. 147–197, Springer Berlin Heidelberg, ISBN 978-3-642-13914-7, https://doi.org/10.1007/978-3-642-13914-7_5, 2012.

Yang and Slingo: The Diurnal Cycle in the Tropics, Monthly Weather Review, 129, 784–801, https://doi.org/10.1175/1520-0493(2001)129<0784:TDCITT>2.0.CO;2, 2001.

https://doi.org/10.5194/egusphere-2026-1019
Preprint. Discussion started: 10 March 2026

Yokoi, S., Mori, S., Katsumata, M., Geng, B., Yasunaga, K., Syamsudin, F., Nurhayati, and Yoneyama, K.: Diurnal Cycle of Precipitation Observed in the Western Coastal Area of Sumatra Island: Offshore Preconditioning by Gravity Waves, Monthly Weather Review, 145, 3745–3761, https://doi.org/10.1175/MWR-D-16-0468.1, 2017.

Zhao, W., Huang, Y., Siems, S., and Manton, M.: A characterization of clouds over the Great Barrier Reef and the role of local forcing, International Journal of Climatology, n/a, https://doi.org/10.1002/joc.7660, 2021.